MOLECULAR PHYSICS, 1996, VOL. 89, NO. 1, 139–156

Ab initio study of the individual interaction energy components in the ground state of the mercury dimer

By CHRISTIAN F. KUNZ, CHRISTOF HÄTTIG and BERND A. HESS
Institut für Physikalische und Theoretische Chemie, Universität Bonn, Wegelerstr. 12, D-53155 Bonn, Germany

(*Received 2 January 1996; accepted 8 February 1996*)

Relativistic and non-relativistic all-electron, *ab initio* methods are used to investigate the role of the individual energy components in the total interaction energy involved in the formation of the weakly bound ground state $X\ ^1\Sigma_g^+$ of the Hg_2 molecule. The interaction energy is partitioned according to a hybrid approach into a supermolecular repulsive potential and the damped dispersion energy derived from perturbation theory. Both parts are then computed individually and their dependence on relativity and electron correlation investigated. From this analysis, hybrid potentials that comprise different physical interactions are constructed and the importance of specific features is evaluated by comparison of the appropriate hybrid potentials with each other and with the experimental curve. The most detailed model is based on a CASSCF supermolecular potential to which the damped intramonomer correlated dispersion energy series is added. In the relativistic case it yields a potential with quantitatively correct asymptotic behaviour and which is able to predict potential parameters that agree reasonably well with the experimental results. The asymptotic density method developed by Duman and Smirnow was tested as an inexpensive alternative for the calculation of the repulsive part of the hybrid potential. In spite of its recent success in the calculation of the He–He potential, it cannot provide a good repulsive component in the case of Hg_2. As a result of this work, this failure can be attributed to the unusually strong induction effects in the ground state mercury dimer bond, which lower repulsive forces substantially.

1. Introduction

The mercury dimer in the $X\ ^1\Sigma_g^+$ ground state is a weakly bound van der Waals molecule due to the closed-shell character of the mercury atom monomers. Since its first investigation more than seventy years ago [1] it has remained a vividly debated topic up to the present time. The unusually strong interest in the molecule comes partly from its practical significance [2, 3] and partly from the challenge it still provides for theoretical methods. A considerable number of works have been published covering experimental [4–16] and theoretical semiempirical [17] as well as *ab initio* studies [18–28] of the ground and excited states of the Hg_2 molecule.

In the effort towards a theoretical description of the ground state of Hg_2 a number of different approaches have been tested including variants of the Gordon–Kim method [18–21], DFT calculations [22–24, 28] and other *ab initio* standard techniques [25–27]. In spite of this, no satisfactory description of the weak Hg—Hg bond in the ground state has yet been achieved, even in the case of highly correlated methods (CCSD(T), MBPT4) as applied by Schwerdtfeger *et al.* [27]. The inaccuracy of previous calculations is seen through comparison of the predicted potential parameters with the results of recent highly accurate experiments [29–32].

Why does the conceptually simple diatomic Hg_2 still present a problem for today's

0026–8976/96 $12·00 © 1996 Taylor & Francis Ltd

theoretical methods? Partially, the problems derive from technical difficulties that the specific features of Hg_2 pose for *ab initio* calculations. The large number of electrons ($n_e = 160$) requires huge basis sets in all-electron calculations, the ground state bonding energy in the mercury dimer is very small, both intra- and intermonomer correlation effects play a dominating role in the dimer, which is not bound at the (Dirac)–Hartree–Fock ((D)HF) level of theory and, finally, strong relativistic effects have to be taken into account, whose role in interatomic interactions is not yet fully clear. Consequently, only highly accurate, post-HF methods that account for relativistic effects should have a chance to yield reliable results. These technical difficulties, however, still do not explain the intrinsic physical problems of this interesting molecule.

Our goal in the present study was twofold. First, we wanted to get a deeper understanding of the physics involved in the formation of the ground state mercury dimer bond. This is equivalent to the partitioning of the interaction energy into several components, which can be attributed to different physical interactions, and evaluating the dependence of these parts from basic effects such as correlation and relativity. In a second step, the detailed results were to be used to explain, as far as possible, the physical reasons for the failure of the previous calculations, and clarify special questions, e.g., about the overall strength of relativistic effects in the bonding energy.

To assure model-independence and reliability of the results, all calculations have been carried out with all-electron *ab initio* methods, that produced very accurate results in the past. For a further check, all results were compared with experimental data, as far as available.

In the description of weakly bound systems within the framework of the Born–Oppenheimer approximation mainly two complementary types of methods are used. The straightforward approach consists of the application of standard variational techniques on the van der Waals complex, which is treated as an ordinary molecule. Calculations carried out in this fashion are referred to normally as supermolecular calculations [33]. Alternatively, a perturbative approach using one of the various formulations of symmetry adapted perturbation theories (SAPT), e.g., the Murrel–Shaw–Musher–Amos (MSMA) [34, 35] or the symmetrized Rayleigh–Schrödinger (SRS) [36] methods, may be used. For a recent review of perturbation theory applied to intermolecular interactions, see [37].

Both supermolecular and perturbative approaches have their advantages and disadvantages, leading to different problems in the practical calculation of van der Waals molecules. In a supermolecular calculation difficulties arise in the computation of the correlation energy, whose dispersion contributions call for large basis sets including dispersion functions with high angular momenta. On the other hand, one of the main problems in SAPT calculations is the calculation of exchange and higher than second-order terms. As was pointed out by Buckingham [38] and others, these specific problems may be circumvented by the use of a so called hybrid approach. In the hybrid approach the total interaction energy is partitioned into a sum of two parts, where one is obtained through a supermolecular and the other through a perturbative calculation. Clearly, the two parts of a hybrid potential must include only entirely separated entities of the interaction energy, in order to avoid double counting of single energy components. The commonly used partitioning is given by

$$V(R) = V_{\text{supermol}} + V_{\text{disp}}, \tag{1}$$

where V_{disp} is the damped dispersion series from ordinary London theory. The

dispersion energy is a pure (dynamic) intermonomer correlation energy, and constitutes the leading attractive term in complexes of unpolar monomers. In the asymptotic region it can be derived through a multipole expansion of the interaction potential, whereas damping functions have to be included at shorter distances to allow for charge-overlap effects. Intramonomer correlation enters the dispersion energy in the form of correlated dispersion coefficients.

The most frequently used supermolecular part in the hybrid approach is either a supermolecular SCF–Heitler–London (HL) or an SCF potential. The HL energy includes all first-order effects that arise in SAPT theories, i.e., first-order electrostatic and exchange energy. A SCF potential, moreover, comprises induction effects of all orders, which are not accounted for in the HL potential. Induction effects therefore can be calculated by subtracting the HL from the SCF energy. The difference is dominated by the second-order induction and exchange induction but contains also higher than second-order terms, and caution must be applied in its interpretation [39, 40]. Since neither the HL nor the SCF supermolecular energies contain any correlation energy, a hybrid potential built with these is safe as concerns double-counting of any contribution. Hybrid potentials constructed in this way were found to give good results for several systems [41, 42]. In spite of this, neither a HL nor a SCF plus damped dispersion energy hybrid potential leads to satisfactory results in the case of the mercury dimer (see section 4), and one has to seek better approximations.

The error in a HL or SCF plus dispersion potential has two sources. First, the potentials omit the exchange-dispersion and higher-order dispersion energy effects. However, these were found to be negligible for most of the van der Waals complexes studied near the potential energy minimum [37, 40]. The main deficiency therefore comes from the omission of intramonomer correlation effects on the supermolecular potential. In terms of perturbation theory, intramonomer correlation alters the interaction energy components included in the supermolecular potential (i.e., first-order electrostatic and exchange plus induction effects of all orders) via changes in the electron density and the polarizability. Though the problem is perfectly clear from a perturbation theory viewpoint, the inclusion of intramonomer correlation into a supermolecular potential that is to be used as the repulsive part of the hybrid potential is an as yet unsolved task. Since there is no way of identifying the part of the correlation energy in a supermolecular calculation that is attributed to the intramonomer correlation effects in the sense mentioned, it is not clear how the calculation has to be carried out practically. If a correlated supermolecular calculation is performed, it will always contain a fraction of the correlation energy that is already included in the dispersion part of the potential, and therefore double counting inevitably arises upon summation of the dispersion part.

Nevertheless, it is possible to include a part of intramonomer correlation effects into the repulsive potential with only minimal risk of double counting. This is done by taking account of only the static (near-degeneracy) correlation in the supermolecular calculation, bearing in mind that the dispersion energy is mainly a dynamic correlation effect. A way of including only static correlation effects is given by a CASSCF calculation with a small active space consisting of the near degenerate 6s and 6p orbitals. Clearly, not the whole consequences of correlation in the sense stated above can be dealt with by this method, but in any case the correlation effects are not overestimated by double counting after addition of the dispersion series. That means a hybrid potential based on a supermolecular CASSCF potential should give a systematically better approximation than one in which a SCF potential is used.

A very promising alternative for the calculation of the interaction energy of two atoms has been developed by Duman and Smirnov [43] and applied recently with success to the He dimer potential [44]. In this approach the basic partitioning of the interaction energy into the dispersion and repulsive potential parts is the same as in the hybrid model, but the repulsive part is calculated in a different fashion. Instead of using a supermolecular calculation, the repulsive potential including first-order effects plus exchange-dispersion contributions is computed from the monomers asymptotic electron density via the surface integral method [45, 46] taking account of the exchange of only one monomer electron at a time. Since only monomer information is required for the calculation of the interaction potential, the ansatz is basically perturbative in nature.

The method involves two major advantages compared with the conventional hybrid approach. First, an expensive supermolecular calculation is not required, reducing the cost of the calculation considerably and, second, intramonomer correlation effects can be taken into consideration into the repulsive part easily without any risk of double counting. Regarding the energy components that enter the potential, the results obtained from the Duman–Smirnow method using the SCF monomer density should be comparable with an HL plus dispersion potential. Induction effects, that derive from the distortion of the monomers electron distribution are not included in the interaction energy.

This method is restricted to the interaction of two closed-shell atoms. We applied it to the mercury dimer, in order to test its performance in this case and to obtain further insight into the physics involved.

In section 2 the employed methods are sketched briefly, and the technical details of the calculations are given in section 3. Section 4 contains the results of our calculations including a detailed discussion.

2. Methods

2.1. *Relativistic effects*

Relativistic effects cannot be omitted from any accurate calculation of systems in which one or more heavy atoms are involved. A very feasible and yet highly accurate method is given by the use of the spin-free no-pair Hamiltonian [47]. It can be derived from the no-pair Hamiltonian [48] by a Douglas–Kroll transformation [49] and averaging out spin components, resulting in a one-component formalism. The spin-free no-pair Hamiltonian contains the relativistic kinetic energy of a free particle and relativistic effective one- and two-particle potentials. The corrections of the two-particle potential had been found to produce negligible effects in the valence-shell energies [50], and thus can be omitted in the calculation of intermolecular interactions. The employed spin-free no-pair Hamiltonian then has the form:

$$H_{+}^{\mathrm{sf1}} = \sum_i E_i + \sum_i V_{\mathrm{eff}}^{\mathrm{sf}}(i) + \sum_{i<j} \frac{1}{r_{ij}}, \tag{2}$$

with

$$E_i = c(p_i^2 + m^2c^2)^{1/2} \tag{3}$$

$$V_{\text{eff}}^{\text{sf}}(i) = -A_i[V_{\text{ext}}(i) + \mathbf{R}_i V_{\text{ext}}(i)\mathbf{R}_i]A_i - W_1^{\text{sf}}(i)E_i W_1^{\text{sf}}(i) - \tfrac{1}{2}[(W_1^{\text{sf}})^2, E_i] \tag{4}$$

$$A_i = \left(\frac{E_i + mc^2}{2E_i}\right)^{1/2} \tag{5}$$

$$\mathbf{R}_i = \frac{c\mathbf{p}_i}{E_i + mc^2}. \tag{6}$$

$W_1^{\text{sf}}(i)$ is an integral operator with the kernel

$$\mathscr{W}_1^{\text{sf}}(\mathbf{p}_i, \mathbf{p}'_i) = A_i(\mathbf{R}_i - \mathbf{R}'_i)A'_i \frac{V_{\text{ext}}(\mathbf{p}_i, \mathbf{p}'_i)}{E_i + E'_i} \tag{7}$$

In a practical calculation using GTO basis sets, relativistic effects can be incorporated by correction of the one-electron integrals involved, at negligible computational cost. The employed matrix method has been discussed extensively in [50].

To examine relativistic effects in the mercury dimer, all calculations were carried out for the relativistic and non-relativistic Hg atom and Hg_2 molecular in a completely analogous fashion, omitting relativistic corrections in the non-relativistic case. This assures direct comparability of the results, leading to a straightforward interpretation of differences in relativistic and non-relativistic bonding components.

2.2. *Calculation of the dispersion series*

The damped dispersion energy series used in the construction of composite potentials has the form

$$V_{\text{disp}} = -\sum_{n=3}^{\infty} \frac{C_{2n} f_{2n}(R)}{R^{2n}}, \tag{8}$$

where the f_{2n} are the appropriate damping functions, given by the expression derived by Tang and Toennies [42]

$$f_{2n}(R) = 1 - e^{-bR} \sum_{k=0}^{2n} \frac{(bR)^k}{k!}. \tag{9}$$

The damping factor b in the functions f_{2n} is calculated from the corresponding repulsive part of the potential, that is to be employed in combination with the dispersion part. In the case of the supermolecular potential it is a constant obtained from a Born–Mayer fit of the repulsive potential into a single exponential function $V_{\text{rep}} = A \exp(-bR)$. The supermolecular damping factors describe the ascent of the repulsive potential, and their values can be employed to interpret the effects on it of relativity, induction and static correlation. When a Duman–Smirnow potential is used, for which an analytical expression is given, a better approximation can be used in the computation of b. Tang and Toennies showed [51] that the best damping factor for a repulsive potential which deviates from the simple exponential form is given by

$$b(R) = -\frac{\mathrm{d}}{\mathrm{d}R} \ln V_{\text{rep}}, \tag{10}$$

and hence for the Duman–Smirnow-potential,

$$b(R) = 2\beta - \frac{\frac{7}{2\beta} - 1}{R}, \tag{11}$$

where β is a simple function of the ionization energy, as explained in the next subsection. Consequently, the damping factor is itself a function of the interatomic distance.

The calculation of the dispersion coefficients is a much more involved task, since it requires knowledge of the dynamic polarizabilities on the imaginary frequency axis. These can be integrated using the Casimir–Polder equation [52], to give the corresponding dispersion coefficients. The first three homoatomic dispersion coefficients are thereby given according to the expressions [38]:

$$C_6 = \frac{3}{\pi}\int_0^\infty \alpha_1^2(i\omega)\,\mathrm{d}\omega \tag{12}$$

$$C_8 = \frac{15}{\pi}\int_0^\infty \alpha_1(i\omega)\,\alpha_2(i\omega)\,\mathrm{d}\omega \tag{13}$$

$$C_{10} = \frac{28}{\pi}\int_0^\infty \alpha_1(i\omega)\,\alpha_3(i\omega)\,\mathrm{d}\omega + \frac{35}{\pi}\int_0^\infty \alpha_2^2(i\omega)\,\mathrm{d}\omega.$$

Uncorrelated dynamic polarizabilities can be calculated employing the TDHF [53–55] method. Correlated frequency-dependent polarizabilities can be obtained by mens of the recently descried TDMP2 [56] method. The derived dispersion coefficients will be referred to in the following as uncorrelated and correlated dispersion coefficients, respectively. Since higher-rank polarizabilities are increasingly tedious to obtain, one can use recurrence relationships to calculate higher dispersion coefficients, once the C_6, C_8, C_{10} are known. It should be noted, however, that errors in the lower dispersion coefficients are magnified in each extrapolation step, and it is unwise to stress the recurrence formulae too much.

2.3. *Duman–Smirnow method*

In the Duman–Smirnow method the repulsive potential including first-order electrostatic, exchange and second-order exchange-dispersion for the interaction of two closed-shell atoms with an s^2 valence configuration is given analytically by [44]

$$V_{\mathrm{DS}} = D R^{\frac{7}{2\beta}-1}\exp(-2\beta R), \tag{14}$$

where β is a simple function of the ionization energy $\beta = (2\varepsilon_{\mathrm{IE}})^{1/2}$, and D is computed according to

$$D = A^4 \frac{\Gamma\left(\frac{1}{2\beta}\right)}{2^{\frac{1}{\beta}+1}\beta^{\frac{1}{2\beta}+2}}\int_0^1 \exp\left(\frac{y-1}{\beta}\right)(1-y)^{3/2\beta}(1+y)^{1/2\beta}\mathrm{d}y. \tag{15}$$

The factor A be calculated approximately from the asymptotic electron density of the Hg atom with

$$A(r) = \lim_{r\to\infty}\left(\frac{2\pi\rho(r)\exp(2\beta r)}{r^{\frac{2}{\beta}-2}}\right)^{1/2}. \tag{16}$$

The factor 2 in the numerator of the root is correct only for RHF wavefunctions, and should be slightly smaller in correlated wavefunctions due to radial correlation [57]. The introduced error, however, should be very small compared with the error in the calculation of the density, and can be neglected safely.

3. Technical details of the calculations

3.1. *Supermolecular calculations*

All-electron supermolecular calculations for the relativistic and non-relativistic ground state mercury dimer were carried out on the SCF-HL, SCF and CASSCF levels using the 'Molcas-2' program package [58]. In the CASSCF calculations the active space was chosen as the subspace spanned by the 6s and 6p orbitals. The calculations were performed using C_{2v} symmetry. All results have been BSSE corrected using the function-counterpoise scheme from Boys and Bernardi [59]. The Hg—Hg separation interval extends from $5\,a_0$ to $12\,a_0$ (a_0 = bohr $\approx 5{\cdot}291\,77 \times 10^{-11}$ m). Relativistic effects were included as described above.

In the relativistic case the basis set reported by Gleichmann and Hess [60] was used. In order to guarantee direct comparability of relativistic and non-relativistic results, an analogous basis set was constructed for the non-relativistic mercury atom, starting from the same primitive basis and contracting it using non-relativistic MO coefficients.

After calculation of the supermolecular potentials, these were fitted in a single-exponential form in order to recover the Born–Mayer damping factors. To accomplish this, the counterpoise-corrected potential energies were employed in the separation interval 5–10 a_0 for the HL and SCF curves and 5–8·5 a_0 in the CASSCF cases, where energies at larger separations deviate substantially from the simple exponential model.

3.2. *Polarizability-optimized basis sets of the Hg atom and homonuclear dispersion coefficients for Hg_2*

The basis sets for the calculation of the polarizabilities in the relativistic and non-relativistic cases were obtained upon simultaneous optimization of the static dipole, quadrupole, and octupole polarizabilities of the relativistic and non-relativistic mercury atom at the CPHF level of theory. This was done starting from the basis sets employed in the supermolecular calculations and successively decontracting the diffuse d and f orbitals and adding polarization functions to the basis sets until saturation in the three quantities α_1, α_2, α_3 was observed. Knowledge of the most easily polarizable orbitals gives a guide for the systematic construction of polarizability-optimized basis sets [61–64]. By freezing appropriate orbitals in the polarizability calculations, the 6s orbital was found to be responsible for most of the polarizability in both the relativistic and non-relativistic mercury atom, followed by the 5d orbitals. All other orbitals produced nearly negligible contributions, but were nevertheless taken into account in subsequent calculations. The resulting basis sets for the calculation of dynamic polarizabilities at imaginary frequencies can be characterized as follows. In the relativistic case the basis from Gleichmann and Hess with the following modifications was used. The most diffuse two d and one f functions were decontracted and three d, three f and two g functions with exponents 0·064, 0·026, 0·01 (d), 0·08, 0·03, 0·01 (f), 1·0, 0·4 (g) were added, leading to the scheme (21s17p13d10f2g)/[14s11p10d7f2g]. In the non-relativistic case the same modifications regarding d and f

orbitals were found to produce the best results. However, three g functions with exponents 2•4, 1•0, 0•4 had to be included in order to reach the same degree of saturation in the octupole polarizabilities as in the relativistic case. The contraction scheme is therefore (21s7p13d10f3g)/[14s11p10d7f3g].

After the optimization of the static polarizabilities, the dynamic dipole, quadrupole, and octupole polarizabilities α_1, α_2, α_3 were calculated on a grid of imaginary frequencies on TDHF and TDMP2 levels for both the relativistic and the non-relativistic mercury atom. From these, uncorrelated and correlated C_6, C_8, C_{10} dispersion coefficients were obtained through a numeric Gauss–Chebyshev integration of the Casimir–Polder equation. The integration was carried out with a varying number of gridpoints (5, 10 and 15 at frequencies between 0 and 19•1 au) in order to examine the convergence behaviour. The C_6, C_8 and C_{10}-coefficients were found to have converged using 15 grid points in the integration and, consequently, these values were used in the following. The results for the static correlated and uncorrelated polarizabilities and dispersion coefficients are shown in table 1.

In the calculation of higher dispersion coefficients we employed the formulae derived from Douketis *et al.* [41],

$$\frac{C_{12}}{C_6} = \frac{17280}{16807}\left(\frac{C_{10}}{C_8}\right)^3, \tag{17}$$

$$\frac{C_{14}}{C_6} = \frac{818741}{839808}\left(\frac{C_{12}}{C_{10}}\right)^3, \tag{18}$$

for the C_{12} and C_{14} coefficients and the more general formula of Tang and Toennies [65],

$$\frac{C_{n+4}}{C_{n-2}} = \left(\frac{C_{n+2}}{C_n}\right)^3, \tag{19}$$

for all higher dispersion coefficients.

Once the repulsive part and the dispersion coefficients are known, the only question regarding the dispersion series is, the order to which the series must be calculated. If it is truncated at too low an order, substantial bonding components may be lost. On the other hand, if the dispersion series is carried out too far, there may be a risk of introducing numerical errors from inaccurate higher-order dispersion coefficients. The problem was solved as follows. All supermolecular hybrid potentials were built in a first step using only the first three terms in the dispersion series with correlated dispersion coefficients and the appropriate Born–Mayer damping factors. Then, higher dispersion terms were added successively to the hybrid potentials until the bonding energy had converged. This turned out to be the case after the $1/R^{16}$ term, and all higher terms thereafter were neglected. Consequently, only C_{12}, C_{14} and C_{16} dispersion coefficients had to be calculated using recurrence formulae.

3.3. *Calculation of the Duman–Smirnow parameters*

The Duman–Smirnow repulsive potential is a two-parameter function in which A is rather difficult to obtain, because the electron density in a region not sensitive to standard variational methods is needed. Two approaches based on variational methods may be used for its calculation. The first consists of numerical computation and is restricted to atoms and small molecules. In the second, one can try to calculate

Table 1. Correlated and uncorrelated static polarizabilities for Hg and dispersion coefficients for Hg_2

	Rel.	Ref.	Non-rel.	Ref.	Exp.
α_1^{SCF}	45·258	40.69[a]; 44·74[b]	81·205	80[c]; 79·27[a] 81·38[b]	—
α_2^{SCF}	336·69	—	855·12	—	—
α_3^{SCF}	5983·4	—	18878	—	—
α_1^{MP2}	28·56	28·67[d]; 26·33[a] 32·8[f]	45·24	48·39[a];47·10[d]	34 ± 1[e]
α_2^{MP2}	178·7	243·2[f]	399·6	—	—
α_3^{MP2}	2040	3010[f]	4198	—	—
C_6^{TDHF}	448·6	—	888·3	—	—
C_8^{TDHF}	18236	—	54133	—	—
C_{10}^{TDHF}	978200	—	3958000	—	—
C_6^{TDMP2}	293·2	222·4[f]; 240[g]	481·1	—	290[h]
C_8^{TDMP2}	9657	9602[f]	23355	—	—
C_{10}^{TDMP2}	381200	443100[f]	1135000	—	—

[a] MP2 [64].
[b] SCF [27].
[c] Numerical HF, polarization of the 6s orbital [74].
[d] MP2 [27].
[e] P. Wüsthoff [71].
[f] CI, 2 VE-PP, STO-basis.
[g] Fit to optical dispersion of Hg vapour [73].
[h] From gas viscosity [72].

the asymptotic density via basis set methods, where STO basis sets definitely should give better results, since they show the right asymptotic behaviour. However, we wanted to test the performance of Gaussian-type basis sets in order to check whether a computation of the A factor is in principle possible in this way. Hence, both numerical and basis set methods using a suitable GTO basis were applied, and finally converged to nearly identical results. This gives rise to the hope that the Duman–Smirnow method may be extended to calculations of intermolecular potentials as well.

In every case, the A factor can be calculated only simultaneously with the second Duman–Smirnow parameter β using formula (16) to calculate the function $A(r)$ and varying β to give a nearly constant value of A for large separations from the nucleus. If instead the value for β that is obtained from a calculation of the ionization energy by the same method as employed in the computation of the density is used, the asymptotic value of $A(r)$ is found either to converge rapidly to zero or to diverge. This is because the approximately calculated density and ionization energy in general do not display the same relationship as in the exact case. However, the optimized value for β is always near to the calculated one and may be used as a good starting value in the optimization. The stable distance range for the computation of A was found to extend from 6 a_0 to 20 a_0 in the case of numerical calculations of the density. In basis set calculations the upper border for the stable distance range is considerably lower (only 8 a_0), reflecting the fact that GTO basis sets fall off too quickly for large distances from the origin. In the region below 6 a_0 the density is determined substantially by the core in both calculations, and a rapidly decreasing function $A(r)$ is found therein.

Numerical calculation of the electron density was carried out with the program 'Grasp' [66] on Dirac–Fock (DF) and multi-configuration Dirac–Fock (MCDF) levels with two ($[Xe]4f^{14}5d^{10}6s^2$, $[Xe]4f^{14}5d^{10}6p^2$) and four ($[Xe]4f^{14}5d^{10}6s^2$, $[Xe]4f^{14}5d^{10}6p^2$, $[Xe]4f^{14}5d^{9}6s^{2}6p^1$, $[Xe]4f^{14}5d^{9}6s^{1}6p^2$) non-relativistic configurations. In the non-relativistic case the speed of light was increased to 10^6 times its normal value.

Calculations of the asymptotic electron density with GTO basis sets were carried out only for the relativistic atom. This was done on SCF, CASSCF and SDCI levels using the 'Molcas-2' program and relativistic corrections with the spin-free no-pair Hamiltonian. We started with the basis set from Gleichmann and Hess, which produced a stable value for A on the SCF level but not on any correlated level. To this basis, even-tempered s functions were added and the calculations repeated until the differential density in the long distance region relative to the previous calculation vanished. Three additional s functions with exponents 0·005, 0·002, 0·001 were found to suffice for this purpose, and with this basis set a stable value of A could be obtained on both SCF and CASSCF levels. The SCF A value remained the same in the course of the calculations.

4. Results and discussion

4.1. *Properties of the mercury atom*

Relativistic and intramonomer correlation effects have nearly an equally strong effect on the polarizabilities of the mercury atom, both roughly halving their values in the static case. This result is in perfect agreement with previous calculations of the dipole polarizability of Hg [27, 64] that, however, do not investigate higher-rank polarizabilities and higher-order dispersion coefficients. As a consequence of the similar strength of correlation and relativity, uncorrelated relativistic and correlated non-relativistic dispersion coefficients are very similar. Correlation in the non-relativistic case has a slightly more pronounced effect, partially from the smaller energetic separation of the 6s and 6p orbitals. The results for the static polarizabilities and the dispersion coefficients can be found in table 1. It should be noted, that the TDMP2 method overestimates correlation effects on polarizabilities and the TDMP2 dispersion energy thus may be systematically too weak. A first hint can be seen in the fact that the experimental value for the dipole polarizability lies in between the TDHF and TDMP2 values. As well as the total value of the polarizabilities, the contribution of single orbitals is noteworthy. For a direct interpretation in terms of orbital polarizabilities an UCHF calculation has to be performed, since only in this method does the sum of the orbital contributions give the total polarizability. It is found that in the relativistic case the 5d shell contributes considerably more to the total polarizability, making up, e.g., a fraction of roughly 20% in the case of the dipole polarizability, in contrast to roughly 10% in the non-relativistic case.

What is the reason for these phenomena? First of all lowering of polarizabilities as a consequence of correlation is a rather peculiar feature. In the case of the mercury atom it can be attributed to the near-degeneracy of the 6s and 6p orbitals. In contrast to the usual trends, this makes the electron distribution more compact upon inclusion of correlation and additionally lowers polarizability through partial occupancy of the 6p orbitals.

Relativistic effects can be pictured in an analogous fashion. Here the contraction of the 6s orbital accompanied by the inflation of the 5d shell (among others) leads to a smaller total polarizability, but raises the relative contribution of the 5d shell. To

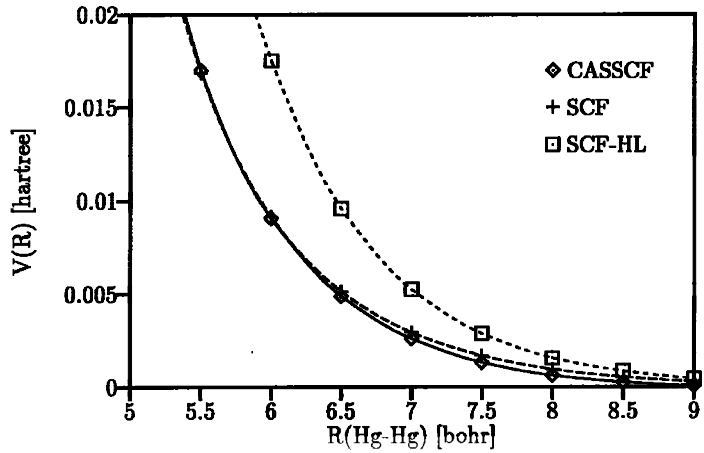


Figure 1. Relativistic supermolecular potentials.

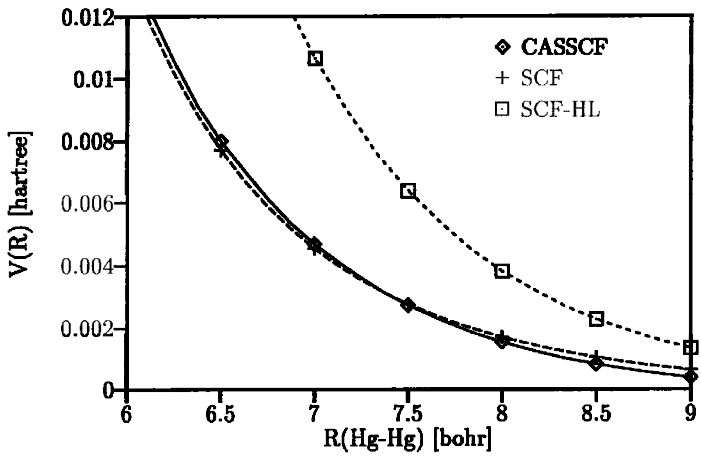


Figure 2. Non-relativistic supermolecular potentials.

Table 2. Born–Mayer factors for relativistic and non-relativistic supermolecular potentials.

Potential	A(rel)	b(rel)	A(non-rel)	b(non-rel)
HL	28·113	1·228	14·178	1·028
SCF	11·442	1·179	7·823	1·050
CAS	24·488	1·316	13·988	1·144

support this view, the $\langle r^2 \rangle$ mean values for the important orbitals and the whole atom were calculated on correlated and uncorrelated levels and found to be in agreement with our interpretation.

4.2. *Repulsive supermolecular potentials*

The calculated supermolecular potentials are shown in figures 1 and 2, the Born–Mayer factors obtained from these are listed in table 2. All potentials are, as expected, purely repulsive in the whole interatomic separation range. In the relativistic

SCF case the result obtained is nearly identical with that of Pyykkö [27, 67], who used a 20 VE relativistic PP-SCF. This shows that the chosen basis contains enough diffuse functions to allow an accurate description of the charge-overlap effects.

In a comparison of the three potentials in a series (i.e., relativistic or non-relativistic), the first thing to be noted is the striking difference in the HL and SCF potentials. This shows that induction effects play a prominent role in the stabilization of the mercury dimer, in contrast to the situation commonly encountered. In the vast majority of van der Waals complexes of unpolar monomers [39, 68, 69] the difference between the HL and SCF potentials is very small, and often can be neglected. There are two reasons: first, the attractive induction energy is compensated largely by the repulsive exchange-induction energy, typically by 90% ; second, the induction energy itself is only so large that the sum of second-order contributions (i.e., the remaining 10%) is of no significance. Hence, the abnormal strength of induction effects in the mercury dimer may come from a deficiency in compensation of induction energy through exchange or, alternatively, from a very large induction energy itself. To investigate further, we computed the short-range non-multipole-expanded induction energy without exchange effects on UCHF and CPHF levels, and indeed found it to be roughly ten times larger than the difference $E_{SCF} - E_{HL}$. Consequently, cancellation of the induction energy through exchange effects takes place exactly as in other cases, and the abnormally large value of the induction energy is responsible for the difference in the SCF and HL potentials. Since the short ranging induction effects in the mercury dimer lead to a considerable energy lowering, the mercury dimer may regarded as a case in between a weakly bound van der Waals molecule and a chemically bound species. In the light of this interpretation it becomes clear why the early Gordon–Kim method [18–21] failed to deliver a proper description of the mercury dimer: It cannot cope with induction effects, since it involves the assumption of unperturbed monomer densities. At this stage of the investigations we became aware that the Duman–Smirnow method should yield an equally poor performance in the case of the mercury dimer for the same reason. Finally, it should be noted that induction energies play nearly the same role in the relativistic and non-relativistic cases, and are not a special feature of relativity.

The effect of static correlation can be seen by comparison of SCF and CASSCF potentials. The CASSCF potentials are steeper (see, e.g. Born–Mayer-factors) and less repulsive at higher interatomic separations. This can be attributed to the contraction of the electron density through static correlation, which gives rise to less far reaching repulsion. The seemingly small difference is nevertheless quite important, and results in doubling bonding energies in both relativistic and non-relativistic hybrid potentials.

Comparing relativistic and non-relativistic potentials of the same kind, the total repulsion in the non-relativistic case is found to be much larger at all considered distances than its relativistic counterpart. The main reason is to be found simply in the more diffuse non-relativistic 6s orbital, leading to higher overlap in this region. The situation should be reversed for smaller separations, where the denser relativistic electron distribution comes into play.

4.3. *Dispersion energy*

The effect of intramonomer correlation on the dispersion series is expressed through modifications in the dispersion coefficients and the damping factor. Thus, the total action of electron correlation on the attractive energy, as far as included in the

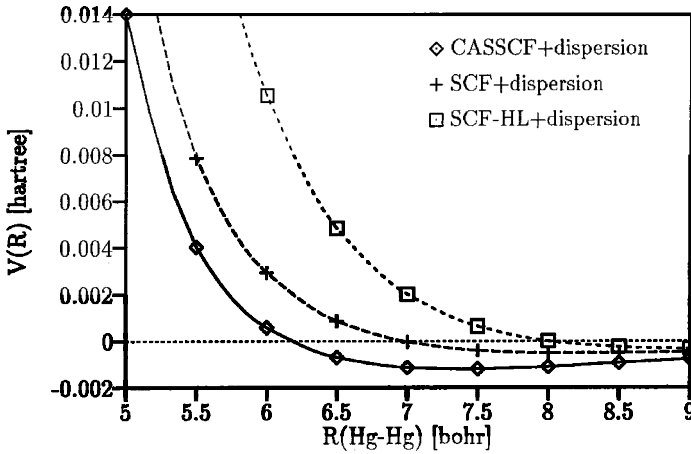


Figure 3. Relativistic hybrid potentials.

ansatz, may be seen through comparison of the dispersion series calculated with the uncorrelated dispersion coefficients and the damping factor from the SCF potential with the series obtained through correlated dispersion coefficients and the CASSCF damping factor. We call these series monomer-uncorrelated and monomer-correlated dispersion energies, respectively. In both the relativistic and non-relativistic case the ratio of correlated and uncorrelated dispersion energy is only a slowly varying function of the internuclear separation In the relativistic case the dispersion energy is diminished by roughly a third through correlation effects, in the non-relativistic case by approximately a factor of two. Comparing uncorrelated dispersion energies for the relativistic and non-relativistic cases, one finds that the relativistic value is also smaller by roughly one half. The difference is substantially smaller when monomer-correlated dispersion energies are compared. Here the relativistic monomer-correlated dispersion energy at 5 a_0 already makes up $\approx 80\%$ of the non-relativistic one. Clearly, relativistic and correlation effects both tend to diminish the dispersion energy but are not additive, and thus lead in their sum to more similar results.

4.4. *Hybrid potentials with supermolecular repulsive part*

Starting from a given supermolecular potential, a hybrid potential can be constructed by adding the dispersion series from either correlated or uncorrelated dispersion coefficients. The standard choice is to use correlated dispersion coefficients, since these provide a systematically better approximation from an *ab initio* viewpoint. However, the uncorrelated dispersion series can be employed to examine the role of intramonomer correlation in the bond. Hybrid potentials, in which correlated dispersion coefficients were used, are shown in figures 3 and 4, and the corresponding parameters in table 3. It can be seen that potential parameters gradually improve as induction and static correlation effects are taken into account. The relativistic CASSCF bonding energy shows agreement within 1 kJ mol^{-1} compared with the experimental result, the equilibrium separation is overestimated by 0·6 a_0. The model thus describes a slightly too loose bond, referring both to energy and to bond distance. This leads to the conclusion that bonding contributions are lacking or are partially underestimated. Rejecting minor corrections from consideration, e.g., dynamic correlation effects on the monomers electron distribution, the deficiency may have two

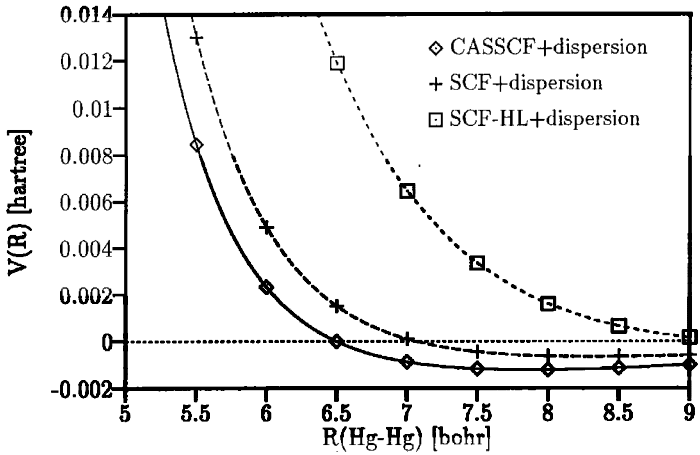


Figure 4. Non-relativistic hybrid potentials.

Table 3. Potential parameters for Hg_2 of hybrid potentials built with monomer-correlated dispersion energy.

	D_e/mE_h	D_e/kJ mol^{-1}	R_e/a_0
Non-relativistic			
HL + dispersion	0·177	0·46	11·3
SCF + dispersion	0·655	1·72	8·35
CASSCF + dispersion	1·22	3·20	7·88
Relativistic			
HL + dispersion	0·335	0·88	9·23
SCF + dispersion	0·520	1·37	8·00
CASSCF + dispersion	1·21	3·18	7·44
Exp.	1·59	4·17	6·86

main reasons. The dispersion series could have been truncated at a too low order or the correlated dispersion coefficients could be too small. Regarding the overestimation of correlation effects on the polarizabilities by the TDMP2 method, the second reason is probably decisive. This view is supported by the observation that the bond is predicted as much too tight when uncorrelated dispersion coefficients are used. The assumption could be tested further by employing more sophisticated correlated dispersion coefficients, but these are not available at present.

The hybrid potential that comprises all correlation effects is built by the CASSCF energy and the monomer-correlated dispersion series. On the other hand, the hybrid potential obtained through addition of the monomer-uncorrelated dispersion energy to the SCF potential includes no intramonomer correlation. The influence of the latter may therefore be seen by comparison of these potentials. In the relativistic dimer, the monomer-uncorrelated bonding energy is found to be 8·9 kJ mol^{-1} at an equilibrium separation of 6·3 a_0. In the non-relativistic case the corresponding values are 24·4 kJ mol^{-1} and 5·94 a_0, respectively. This shows how sensitive the potential parameters are to the inclusion of intramonomer correlation. Without consideration of intramonomer correlation, very different potential parameters would occur, predicting a much too strongly bound molecule.

Table 4. Duman–Smirnow parameters for the relativistic Hg atom obtained from densities calculated by basis set methods.

Method	Active space	A	D	β
SCF	—	1·85	1·025	0·81
CAS	[6s6p]	2·33	2·8	0·84

Table 5. Dunman–Smirnow coefficients from densities calculated with numerical methods.

Method	Configurations	A	D	β
Relativistic				
DF	$[Xe]4f^{14}5d^{10}6s^2$	1·85	1·025	0·8095
MCDF	$[Xe]4f^{14}5d^{10}6s^2$, $[Xe]4f^{14}5d^{10}6p^2$	2·27	2·48	0·8385
MCDF	$[Xe]4f^{14}5d^{10}6s^2$, $[Xe]4f^{14}5d^{10}6p^2$, $[Xe]4f^{14}5d^{9}6s^{2}6p^{1}$, $[Xe]4f^{14}5d^{9}6s^{1}6p^{2}$	2·35	2·88	0·85
Non-relativistic				
SCF	$[Xe]4f^{14}5d^{10}6s^2$	1·32	0·26	0·722
MCSCF	$[Xe]4f^{14}5d^{10}6s^2$, $[Xe]4f^{14}5d^{10}6p^2$	1·78	0·88	0·7583
MCSCF	$[Xe]4f^{15}5d^{10}6s^2$, $[Xe]4f^{14}5d^{10}6p^2$, $[Xe]4f^{14}5d^{9}6s^{2}6p^{1}$, $[Xe]4f^{14}5d^{9}6s^{1}6p^{2}$	1·73	0·79	0·7605

The relativistic effects can be seen at various stages by comparing the relativistic and non-relativistic potentials of the same kind. Although at the HL + dispersion hybrid potential level the parameters are quite similar. This originates in the cancellation of the larger repulsion with the larger dispersion in the non-relativistic case. Another result would, however, be obtained upon employment of uncorrelated dispersion coefficients. In the CASSCF hybrid potentials identical bonding energies in the relativistic and non-relativistic case are obtained, though the non-relativistic equilibrium separation is substantially larger.

4.5. *Duman–Smirnow hybrid potentials*

The results for the Duman–Smirnow parameters obtained from the asymptotic electron density of the Hg atom using basis set and numerical methods can be seen in tables 4 and 5. From these, only the more reliable values from numerical calculations were used in the calculation of the repulsive potentials. With these parameters three relativistic and non-relativistic repulsive potentials were calculated, showing different degrees of intramonomer correlation. The uncorrelated Duman–Smirnow potentials (obtained with parameters from the (D)HF calculations) match quite well with the HL repulsive potentials, as was expected for theoretical reasons. Upon consideration of intramonomer correlation the Duman–Smirnow potentials become steeper, again reflecting contraction of the monomer wavefunction.

From the repulsive potentials, hybrid potentials were obtained by adding the monomer-correlated dispersion energy series, damped according to equation (11). For the sake of better comparability with conventional hybrid potentials, the dispersion series in the Duman–Smirnow hybrid potentials was truncated at the same order as in the conventional case. All values of the potential parameters lie close to those of the

Table 6. Potential parameters of Duman–Smirnow hybrid potentials built with monomer-correlated dispersion energies.

	D_e/mE_h	D_e/kJ mol^{-1}	R_e/a_0
Non-relativistic			
DF + dispersion	0·117	0·307	12·00
MCDF (2 config) + dispersion	0·148	0·389	11·72
MCDF (4 config) + dispersion	0·177	0·465	11·37
Relativistic			
SCF + dispersion	0·208	0·546	10·0
MCSCF (2 config) + dispersion	0·226	0·593	9·96
MCSCF (4 config) + dispersion	0·306	0·803	9·46

corresponding HL hybrid potential (see table 6). The hybrid potentials show the expected poor performance, since they cannot deal with the strong induction effects in the mercury dimer. Adding the non-multipole-expanded induction energy from a CPHF or UCHF calculation does not improve the situation, but produces even qualitatively wrong results. The reason lies clearly in the omission of exchange-induction, which still has to be accounted for.

From these results it may be seen that the Duman–Smirnow method can provide an efficient approximation for systems that are described well at the HL + dispersion energy level. It is, however, inappropriate for the discussion of the $X\ ^1\Sigma_g^+ Hg_2$ system, and probably for other cases in which induction energies are of considerable size, i.e., involving highly polarizable monomers.

5. Conclusion

The large difference in the HL and SCF supermolecular potentials of the ground state mercury dimer shows that induction contributions to the bonding energy are essential. The unusually strong induction energy is, as in most other cases investigated, widely cancelled by the exchange-induction. The difference $E_{ind} - E_{exc\text{-}ind}$ is, however, still large enough to make a strong bonding contribution. The picture of the mercury dimer as a van der Waals complex should therefore be modified. It is probably better thought of as an intermediate between a pure van der Waals molecule and a chemically bound species.

Intramonomer correlation and relativistic effects both decrease the dispersion attraction, but their effect is not additive. The dispersion interaction under consideration of electron correlation in the monomers is much more similar in the relativistic and non-relativistic case than without electron correlation. Combined with the stronger first-order repulsion in the non-relativistic case, which has its origin in the more diffuse 6s orbital, very similar relativistic and non-relativistic bonding energies arise, as at the HL + dispersion level of the hybrid potentials. These become even more similar when induction and static correlation effects in the supermolecular potentials are included.

The Duman–Smirnow method has been shown to be a good and inexpensive alternative to an HL supermolecular potential. Since nearly the same potential parameters could be predicted using the density from numerical calculations and basis set calculations with GTO basis sets, the Duman–Smirnow method is likely to be

extendable to molecules as well. In the case of the mercury dimer, a hybrid potential based on a Duman–Smirnow repulsive potential shows poor performance, because it cannot include induction interactions.

We thank P. Pyykkö for providing us with his detailed data. Further we are indebted to G. Jansen for placing his program 'Plotrho' at our disposal. We thank the Deutsche Forschungsgemeinschaft for financial support of this work through the Sonderforschungsbereich 334. Support by the Fonds der Chemischen Industrie is gratefully acknowledged.

References

[1] Frank, J., and Grotian, W., 1922, *Z. Techn. Phys.*, **3**, 194.
[2] Houtermans, F. G., 1960, *Helv. Phys. Acta*, **33**, 933.
[3] Smith, E. W., Drullinger, R. E., Hessel, M. M., and Cooper, J., 1977, *J. chem. Phys.*, **66**, 5667.
[4] Kuhn, H., and Freudenberg, K., 1932, *Z. Phys.*, **76**, 38.
[5] Morozowski, S., 1929, *Z. Phys.*, **55**, 338.
[6] Winans, J. G., 1931, *Phys. Rev.*, **37**, 897.
[7] Winans, J. G., and Heitz, M. P., 1952, *Z. Phys.*, **133**, 291.
[8] Koernicke, E., 1925, *Z. Phys.*, **33**, 219.
[9] Drullinger, R. E., Hessel, M. M., and Smith, E. W., 1977, *J. chem. Phys.*, **66**, 5656.
[10] Hilpert, K., 1982, *J. chem. Phys.*, **77**, 1425.
[11] Epstein, L. F., and Powers, M. D., 1964, *J. phys. Chem.*, **68**, 336.
[12] Hildebrand, J. H., Wakeham, H. R. R., and Boyd, R. N., 1939, *J. chem. Phys.*, **7**, 1094.
[13] Kerr, R. H., and Lund, L. H., 1951, *J. chem. Phys.*, **19**, 50.
[14] Moelwyn-Hughes, E. A., 1951, *J. phys. Chem.*, **55**, 1246.
[15] Carlson, K. D., and Kuschnir, K. R., 1964, *J. phys. Chem.*, **68**, 1566.
[16] Morse, M. D., 1986, *Chem. Rev.*, **86**, 1049.
[17] Maeder, F, and Kutzelnigg, W., 1978, *Chem. Phys.*, **32**, 457.
[18] Gordon, R. G., and Kim, Y. S., 1972, *J. chem. Phys.*, **56**, 3122.
[19] Pyper, N. C., and Gerber, R. B., 1977, *Chem. Phys. Lett.*, **49**, 479.
[20] Clugston, M. J., and Pyper, N. C., 1979, *Chem. Phys. Lett.*, **63**, 549.
[21] Clugston, M. J., and Pyper, N. C., 1978, *Chem. Phys. Lett.*, **58**, 457.
[22] Ballone, P., and Galli, G., 1989, *Phys. Rev.* B, **40**, 8563.
[23] Ballone, P., and Galli, G., 1990, *Phys. Rev.* B, **42**, 1112.
[24] Ortiz, G., and Ballone, P., 1991, *Phys. Rev.* B, **43**, 6376.
[25] Celestino, K. C., and Ermler, W. C., 1984, *J. chem. Phys.*, **81**, 1872.
[26] Balasubramanian, K., Das, K. K., and Liao, D. W., 1992, *Chem. Phys. Lett.*, **195**, 487.
[27] Schwerdtfeger, P., Li, J., and Pyykkö, P., 1994, *Theoret. Chim. Acta*, **87**, 313.
[28] Bastug, T., Sepp, W. D., Kolb, D., Fricke, B., Baerends, E. J., and te Velde, G., 1995, *J. Phys.* B, **28**, 2325.
[29] van Zee, R. D., Blankespoor, S. C., and Zwier, T. S., 1988, *J. chem. Phys.*, **88**, 4650.
[30] Schlauf, M., Dimopoulou-Rademann, O., Rademann, K., Even, U., and Hensel, F., 1989, *J. chem. Phys.*, **90**, 4630.
[31] Zehnacker, A., Duval, M. C., Jouvet, C., Lardeux-Dedonder, C., Solgadi, D., Soep, B., and d'Azy, O. B., 1987, *J. chem. Phys.*, **86**, 6565.
[32] Kredzierski, W., Supronowicz, J., Czajkowski, A., Hinek, M. J., Atkinson, J. B., and Krause, L., 1994, *Chem. Phys. Lett.*, **218**, 314.
[33] van Lenthe, J. H., van Duijneveldt-van de Rijdt, J. G. C. M., and van Duijneveldt, F. B., 1987, *Adv. chem. Phys.*, **69**, 521.
[34] Murrell, J. N., and Shaw, G., 1987, *J. chem. Phys.*, **46**, 1768.
[35] Musher, J. I., and Amos, A. T., 1967, *Phys. Rev.*, **164**, 31.
[36] Jeziorski, B., Chalasinski, G., and Szalewicz, K., 1978, *Int. J. Quantum Chem.*, **14**, 271.
[37] Jeziorski, B., Moszynski, R., and Szalewicz, K., 1994, *Chem. Rev.*, **94**, 1887.
[38] Buckingham, A. D., Fowler, P. W., and Hutson, J. M., 1988, *Chem. Rev.*, **88**, 963.
[39] Jaszunski, M., 1980, *Molec. Phys.*, **39**, 777.
[40] Chalasinski, G., and Jeziorski, B., 1976, *Molec. Phys.*, **32**, 81.

[41] Douketis, C., Scoles, G., Marchetti, S., Zen, M., and Thakkar, A., 1982, *J. chem. Phys.*, **76**, 3057.
[42] Tang, K. T., and Toennies, J. P., 1984, *J. chem. Phys.*, **80**, 3726.
[43] Duman, E. L., and Smirnow, B. M., 1970, *Opt. Spectrosc.*, **29**, 229.
[44] Tang, K. T., Toennies, J. P., and Yiu, C. L., 1995, *Phys. Rev. Lett.*, **74**, 1546.
[45] Herring, C., 1962, *Rev. mod. Phys.*, **34**, 631.
[46] Herring, C., and Flicker, M., 1964, *Phys. Rev.* A, **134**, 362.
[47] Hess, B. A., 1986, *Phys. Rev.* A, **33**, 3742.
[48] Sucher, J., 1980, *Phys. Rev.* A, **22**, 348.
[49] Douglas, M., and Kroll, N. M., 1974, *Ann. Phys.*, **82**, 89.
[50] Samzow, R., and Hess, B. A., 1992, *J. chem. Phys.*, **96**, 1227.
[51] Tang, K. T., and Toennies, J. P., 1992, *Surface Sci. Lett.*, **279**, L203.
[52] Casimir, H. B. G., and Polder, D., 1948, *Phys. Rev.*, **73**, 360.
[53] Olsen, J., and Jorgensen, P., 1995, *Time dependent response theory with applications to self consistent (SCF) and multiconfiguration self consistent field (MCSCF) wave functions* (Aarhus: I.F.A. Print).
[54] McWeeny, R., 1989, *Methods of Molecular Quantum Mechanics*, 2nd Edn (San Diego: Academic Press).
[55] Langhoff, P. W., Epstein, S. T., and Karplus, M., 1972, *Rev. mod. Phys.*, **44**, 602.
[56] Hättig, C., and Hess, B. A., 1995, *Chem. Phys. Lett.*, **233**, 359.
[57] Bardsley, J. N., Holstein, T., Junker, B. R., and Sinha, S., 1975, *Phys. Rev.* A, **11**, 1911.
[58] Fülscher, M. P., Anderson, K., Lindh, R., Malmquist, P. A., Olsen, J., Roos, B. O., Sadlej, A. J., and Widmark, P.-O., 1992, 'Molcas' Version 2.
[59] Boys, S. F., and Bernardi, F., 1970, *Molec. Phys.*, **19**, 553.
[60] Gleichmann, M. M., and Hess, B. A., 1994, *Chem. Phys. Lett.*, **227**, 229.
[61] Almlöf, J., and Taylor, P. R., 1990, *J. chem. Phys.*, **92**, 551.
[62] Sadlej, A. J., 1991, *Theoret. Chim. Acta*, **79**, 123.
[63] Sadlej, A. J., 1991, *Theoret. Chim. Acta*, **81**, 45.
[64] Kellö, V., and Sadlej, A. J., 1995, *Theoret. Chim. Acta*, **91**, 353.
[65] Tang, K. T., and Toennies, J. P., 1978, *J. chem. Phys.*, **68**, 5501.
[66] Dyall, K. G., Grant, J. P., Johnson, C. T., Plummer, E. P., and Parpia, F., 1984, *Comput. Phys. Commun.*, **54**, 425.
[67] Pyykkö, P., private communication.
[68] Chalasinski, G., 1983, *Molec. Phys.*, **49**, 1353.
[69] Mulder, F., van der Avoird, A., and Wormer, P. E. S., 1979, *Molec. Phys.*, **37**, 159.
[70] Maeder, F., and Kutzelnigg, W., 1979, *Chem. Phys.*, **42**, 95.
[71] Wüsthoff, P., 1936, *Ann. Phys.*, **27**, 312.
[72] Hirschfelder, J. O., Curtiss, C. F., and Byrd, R. B., 1964, *Molecular Theory of Gases and Liquids*, 34th Edn (New York: Wiley).
[73] Stwalley, W. C., and Kramer, H. C., 1968, *J. chem. Phys.*, **49**, 5555.
[74] Desclaux, J. P., Laaksonen, L., and Pyykkö, P., 1981, *J. Phys.* B, **14**, 419.